Published in final edited form as:
Mol Cancer Res. 2013 September ; 11(9): 1040–1050. doi:10.1158/1541-7786.MCR-13-0084-T.

Epithelial 11β-hydroxysteroid dehydrogenase type II deletion inhibits *Apc*$^{+/min}$ mouse tumorigenesis via COX-2 pathway inhibition and induction of G1 cell cycle arrest

Li Jiang[1,4], **Shilin Yang**[1], **Huiyong Yin**[1,3], **Xiaofeng Fan**[1], **Suwan Wang**, **Bing Yao**, **Ambra Pozzi**[1], **Xiaoping Chen**[4], **Raymond C Harris**[1], and **Ming-Zhi Zhang**[1,2]

[1]Department of Medicine, Vanderbilt University School of Medicine, Nashville, TN, USA

[2]Department of Cancer Biology, Vanderbilt University School of Medicine, Nashville, TN, USA

[3]Institute of Nutritional Sciences, Shanghai Institute for Biological Sciences, Chinese Academy of Sciences

[4]Heaptic Surgery Center, Tongji Hospital, Tongji Medical College, Huazhong University of Science & Technology, PR. China

Abstract

Cyclooxygenase-2 (COX-2)-derived prostaglandin E_2 (PGE_2) promotes colorectal tumorigenesis. Glucocorticoids are endogenous and potent COX-2 inhibitors, and their local actions are down-regulated by 11β–hydroxysteroid dehydrogenase type II (11ßHSD2)-mediated metabolism. We previously reported that 11ßHSD2 increased in human colonic and *Apc*$^{+/min}$ mouse intestinal adenomas and correlated with increased COX-2 expression and activity, and 11ßHSD2 inhibition suppressed the COX-2 pathway and decreased tumorigenesis. 11ßHSD2 is expressed in *Apc*$^{+/min}$ mouse intestinal adenoma stromal and epithelial cells. We generated *Apc*$^{+/min}$ mice with selective deletion of 11ßHSD2 in intestinal epithelial cells (Vil-HSD2-/- *Apc*$^{+/min}$). 11ßHSD2 deletion in intestinal epithelia led to marked inhibition of *Apc*$^{+/min}$ mouse intestinal tumorigenesis. Immunostaining indicated decreased 11ßHSD2 and COX-2 expression in adenoma epithelia, while stromal COX-2 expression was intact in Vil-HSD2-/- *Apc*$^{+/min}$ mice. In Vil-HSD2-/- *Apc*$^{+/min}$ mouse intestinal adenomas, both p53 and p21 mRNA and protein levels were increased, with concomitant decrease in phosphorylation of retinoblastoma protein, indicating glucocorticoid-mediated G1 cell cycle arrest. Regulated in development and DNA damage responses 1 (REDD1), a novel stress-induced gene that inhibits mammalian target of rapamycin (mTOR) signaling pathway, was increased, while the mTOR signaling pathway was inhibited. Therefore, in Vil-HSD2-/- *Apc*$^{+/min}$ mice, epithelial cell 11ßHSD2 deficiency leads to inhibition of adenoma initiation and growth by attenuation of COX-2 expression, increased G1 cell cycle arrest and inhibition of mTOR signaling as a result of increased tumor intracellular active glucocorticoids. 11ßHSD2 inhibition may represent a novel approach for colorectal cancer chemoprevention by increasing tumor glucocorticoid activity, which in turn inhibits tumor growth by multiple pathways.

Corresponding author: Ming-Zhi Zhang, S-3206, MCN, Vanderbilt University Medical Center, Nashville, Tennessee 37232, USA. Phone: 615.343.1548; Fax: 615.343.2675; ming-zhi.zhang@vanderbilt.edu.

Disclosure of Potential Conflicts of Interest
The authors have no potential conflicts of interest

Keywords

adenoma; epithelia; cyclooxygenase-2; glucocorticoid-metabolism; mice

Introduction

Colorectal cancer (CRC) is a leading cause of cancer death. Most patients present with advanced disease, and metastatic disease remains largely incurable. Therefore, prevention remains the best approach to reduce the overall morbidity and mortality of CRC. There is a clear link between cyclooxygenase-2 (COX-2) derived PGE_2 and CRC progression (1,2) Clinical evidence indicates a 40-50% reduction in CRC in individuals who take NSAIDs regularly, either in the context of sporadic CRC or in patients of familial adenomatous polyposis (FAP) (3-6). NSAIDs reduce the relative risk of CRC primarily due to their ability to inhibit COX-2-mediated prostaglandin production (7). However, long-term use of traditional NSAIDs increases gastrointestinal side-effects due primarily to COX-1 inhibition (8,9) Selective COX-2 inhibitors have shown similar efficacy to traditional NSAIDs in treating acute and chronic inflammatory conditions and in reducing the number and size of adenomas in FAP patients and in $Apc^{+/min}$ mice with fewer gastrointestinal side-effects (10,11), and were touted as promising agents for chemoprevention and chemotherapy of CRC. However, long-term use of selective COX-2 inhibitors has been found to be associated with an increased incidence of cardiovascular events (12,13), thought to be due to inhibition of endothelial cell-derived COX-2 activity, with selective inhibition of COX-2 derived PGI_2 production but without inhibition of COX-1 mediated prothrombotic platelet thromboxane A_2 production (14).

Glucocorticoids (GCs) are the most potent, endogenous, specific COX-2 inhibitors, acting to suppress COX-2, but not COX-1 expression, through stimulating glucocorticoid receptors (15-17). In addition to inhibiting COX-2 expression, GCs also reduce prostaglandin production through inhibition of cytosolic phospholipase A_2 activity, which prevents the release of arachidonic acid from membrane phospholipids (18), and through inhibition of microsomal prostaglandin E synthetase (mPGES-1) expression, a major terminal synthetase in PGE_2 biosynthesis (19). In addition to treatment of hematologic malignancies, GCs can inhibit solid tumor growth, regress tumor mass, and prevent metastasis by blocking angiogenesis (20,21). However, the undesirable side-effects of immune suppression limit their application in cancer chemoprevention and chemotherapy.

In tissues, GC effects are regulated by a “pre-receptor” regulatory mechanism involving 11ß–hydroxysteroid dehydrogenase type I (11ßHSD1) and 11ßHSD2 (12). 11ßHSD1 produces active GCs from inactive metabolites, while 11ßHSD2 converts GCs to their inactive keto-forms. We recently reported that 11ßHSD2 expression was increased in human colonic and $Apc^{+/min}$ mouse intestinal adenomas and correlated with increased COX-2 expression and activity (23). 11ßHSD2 inhibition reduces tumor COX-2-mediated PGE_2 production and tumor growth by increasing the tonic glucocorticoid-mediated suppression of the COX-2 signaling pathway, suggesting that 11ßHSD2 inhibition may be a potential therapeutic option to prevent and/or treat colorectal cancer. To exclude the possible off-targets of glycyrrhizic acid, the 11ßHSD2 inhibitor we used in our previous report (23), and to investigate the role of intestinal epithelial 11ßHSD2 in colorectal tumorigenesis, we generated $Apc^{+/min}$ mouse with selective deletion of 11ßHSD2 in intestinal epithelial cells and determined that 11ßHSD2 in intestinal epithelial cells plays an important role in adenoma development and growth.

Materials and Methods

Generation of a mouse line with selective deletion of 11βHSD2 in intestinal epithelial cells

We utilized a BAC engineering strategy to produce an *Hsd11b2* conditional gene targeting vector, in which a *Neo* cassette was flanked by two *Flrt* sites (Neo^{flrt}), and the *Hsd11b2* gene was flanked by two *lox*P sites ($Hsd11b2^{flox}$). The detailed procedures and information regarding the generation of $Neo^{flrt};Hsd11b2^{flox}$ mice are illustrated in Supplemental Figure 1. The targeting construct was linearized with *Not* I and electroporated into 129 ES cells. The targeting events were found in 6 out of 237 colonies resistant to G418 as demonstrated by an expected 3.0-kb product amplified by PCR and confirmed by Southern blot. Two positive ES clones were used for implantation. Three male chimeras with targeted events (with $Neo^{flrt}/Hsd11b2^{flox}$ allele) were obtained. These chimeras were crossed with female congeneic C57BL/6 mice. Germline transmission of the targeted events in the F1 mice was screened by PCR and further confirmed by Southern blot as illustrated in Supplemental Figure 2. The *Neo* cassette was effectively removed by crossing with ACTB:FLPe mice. The mice bearing the $Hsd11b2^{flox}$ allele were backcrossed to C57BL/6 background for 10 generations, and then crossed with C57BL/6 Vil-Cre mice (Jackson Lab, Stock # 004586), in which the Cre recombinase is controlled by the villin promoter, which is active as early as E12.5 in the entire intestinal epithelium (24).

Animals

All animal experiments were performed according to animal care guidelines and were approved by the Vanderbilt University IACUC. Germline mutations in the adenomatous polyposis coli (APC) gene lead to familial adenomatous polyposis, and inactivation of APC is also found in the majority of sporadic CRC. The $Apc^{+/min}$ mouse generated by random ethylnitrosourea mutagenesis carries a T to A transversion at nucleotide 2549 of the *Apc* gene. The resulting point mutation in codon 850 produces a premature stop codon and a truncated polypeptide of approximately 95 kD (25). The autosomal dominant heterozygous nonsense mutation of the *Apc* gene in the $Apc^{+/min}$ mouse is homologous to human germline and somatic APC mutations. $Apc^{+/min}$ mice develop grossly detectable adenomas within a few months. Vil-Cre/$Hsd11b2^{flox}$ mice were crossed with $Apc^{+/min}$ (C56BL/6, Jackson Laboratory) to generate $Apc^{+/min}$ mice in which the *Hsd11b2* gene in intestinal epithelial cells has been deleted selectively (Vil-HSD2-/- $Apc^{+/min}$ mice). At 20 weeks of age, 10 wild type $Apc^{+/min}$ mice and 8 Vil-HSD2-/- $Apc^{+/min}$ mice were sacrificed for analysis. Under anesthesia with Nembutal (60 mg/kg i.p., Abbot Laboratories), the entire intestine was dissected, flushed thoroughly with ice-cold PBS (pH 7.4), and then filled with fixative (26). The intestine was transferred to 70% ethanol for 24 h, opened longitudinally, and examined using a dissecting microscope to count polyps in a blinded fashion. The tumor diameter was measured with a digital caliper. After tumors were counted, intestinal tissues were processed for paraffin embedding. A subset of mice (6 wild type $Apc^{+/min}$ mice and 6 Vil-HSD2-/- $Apc^{+/min}$ mice) was sacrificed for collection of adenomas and intestine tissue for quantitative real-time PCR, Western blot analysis and determination of tissue levels of corticosterone and 11-keto-corticosterone. All animals were genotyped twice (after weaning and before sacrifice). Probes 0IMR0033, 0IMR0034 and 0IMR0758 were used for $Apc^{+/min}$ genotyping and probes 0IMR0015 and 0IMR0016 for villin-Cre genotyping.

Wild type $Apc^{+/min}$ mice (16-18 weeks of age) were treated with the selective COX-2 inhibitor SC-58236 (2mg/kg/day, daily gastric gavage, a gift from Searle Monsanto) for 7 days and tumors with similar size were collected for Western analysis.

Cell culture

Mouse colon adenocarcinoma MC38 cells (C57BL/6) were obtained from Dr. Bixiang Zhang (Huazhong University of Science & Technology, PR. China) in March, 2012. MC38 cells were authenticated by DNA short-tandem repeat analysis in February, 2012 and used for experiments within 5 months. MC-38 cells were grown in RPMI1640 supplemented with 4,500 mg/l glucose, 2 mM l-glutamine, 10% fetal bovine serum, 100 U/ml penicillin, and 100 μg/ml streptomycin in 5% CO2 and 95% air at 37°C (27). MC-38 cells were cultured in medium with 1% fetal bovine serum overnight and then treated with 1μM dexamethasone or dexamethasone plus 10 μM glucocorticoid receptor antagonist, RU486 in normal culture medium for 6 hours. RU486 was added 30 min before addition of dexamethasone.

RNA isolation and quantitative real time PCR (qRT-PCR)

Total RNA was isolated from tumors using TRIzol reagents (Invitrogen) according to the manufacturer's instructions. qRT-PCR was performed using TaqMan real time PCR machine (7900HT, Applied Biosystems). The Master Mix and all gene probes were also purchased from Applied Biosystems. The probes used in the experiments included mouse S18 (Mm02601778), p53 (Trp53, Mm01731290), p21 (Cdkn1a, 04205640), p27 (Dctn6, 00495994), and REDD1 (Ddit4, Mm00512504).

Measurement of corticosterone and 11-keto-corticosterone

Colonic tissues were collected and stored at −80°C. Tissue levels of corticosterone (active form) and 11-keto-corticosterone (inactive form) were measured using high-performance liquid chromatography coupled with electrospray tandem mass spectrometry (23). Corticosterone was from ICN Biomedicals, and 11-keto-corticosterone was from Steraloids.

Antibodies

Affinity-purified rabbit anti-mouse 11βHSD2 (catalog no. BHSD22-A) was purchased from Alpha Diagnostic International; rabbit anti-murine COX-2 (catalog no. 160106) was from Cayman Chemicals; rabbit anti-c-Myc was from Santa Cruz Biotechnology, rabbit anti-REDD1 was from Lifespan (LC-53286); rabbit anti- $p21^{waf1/cip1}$(29470), rabbit anti-p-Rb (9308), rabbit anti-p-mTOR (2971, Ser2448), rabbit anti-p-p70 S6K (9234), rabbit anti-p-4E-BP1 (9451), rabbit anti-p-S6 ribosomal protein (p-rpS6) (4858, Ser235/236), rabbit anti-cleaved caspase-3 (9661) and mouse anti-cyclin D1 (2926) were from Cell Signaling.

Immunohistochemistry and Western analysis

Immunostaining and western blot analysis were carried out as previously reported (28).

Quantitative image analysis

Immunostaining of β-catenin, cleaved caspase-3 and $p21^{waf1/cip1}$ was quantified using the BIOQUANT image analysis system (R & M Biometrics, Nashville, TN) (23). Bright-field images from a Leitz Orthoplan microscope with DVC digital RGB video camera were digitized and saved as computer files. Contrast and color level adjustment (Adobe Photoshop) were performed for the entire image; i.e., no region- or object-specific editing or enhancements were performed.

Statistical analysis

Values are presented as means ± S.E.M. ANOVA and Bonferroni *t*-test were used for statistical analysis, and differences were considered significant when $P < 0.05$.

Results

Since 11ßHSD2 is primarily localized to epithelial cells in both human colonic and *Apc*$^{+/min}$ mouse intestinal adenomas (23), we generated *Apc*$^{+/min}$ mouse line with selective deletion of 11ßHSD2 in intestinal epithelia by crossing *Apc*$^{+/min}$ mouse with *Hsd11b2*$^{flox/flox}$ mice and villin Cre mice (Supplementary Figures 1&2). *Apc*$^{+/min}$ mice are normally on the C57BL/6 background, and *Apc*$^{+/min}$ mouse adenoma development and growth are sensitive to genetic background (29). We therefore backcrossed *Hsd11b2*$^{flox/+}$ mouse onto C57BL/6 background for 10 generations, then crossed with Vil-Cre mouse (C57/BL/6) and *Apc*$^{+/min}$ mouse to get *Apc*$^{+/min}$ mice with *Hsd11b2*$^{flox/flox}$ alleles (wild type *Apc*$^{+/min}$ mice) or with *Hsd11b*$^{\Delta/\Delta}$ alleles (Vil-Cre/*Hsd11b2*$^{flox/flox}$/*Apc*$^{+/min}$ mice, designated as Vil-HSD2-/- *Apc*$^{+/min}$ mice).

To determine whether colonic 11ßHSD2 expression was decreased in Vil-HSD2-/- *Apc*$^{+/min}$ mice, colonic tissues were collected for Western analysis. As indicated in Figure 1A, colonic 11ßHSD2 levels were markedly decreased in Vil-HSD2-/- *Apc*$^{+/min}$ mice compared to wild type *Apc*$^{+/min}$ mice. As expected, colonic COX-2 levels were also markedly decreased in Vil-HSD2-/- *Apc*$^{+/min}$ mice compared to wild type *Apc*$^{+/min}$ mice (Figure 1B). 11ßHSD2 and COX-2 levels in small intestine were also significantly lower in Vil-HSD2-/- *Apc*$^{+/min}$ mice than wild type *Apc*$^{+/min}$ mice (data not shown).

To investigate whether selective deletion of 11ßHSD2 in intestinal epithelia is associated with functional alterations in glucocorticoid metabolism, intestinal tissues were collected and glucocorticoid levels were measured. As indicated in Figure 1C, intestinal corticosterone levels (active glucocorticoid) were > 10-folds higher in Vil-HSD2-/- *Apc*$^{+/min}$ mice than wild type *Apc*$^{+/min}$ mice (corticosterone: 30.34 ± 12.35 vs. 2.73 ± 0.57 ng/g of wild type *Apc*$^{+/min}$ mice, $p < 0.05$, n = 6 in each group). In contrast, intestinal 11-keto-corticosterone levels (inactive glucocorticoid) were significantly lower in Vil-HSD2-/- *Apc*$^{+/min}$ mice than wild type *Apc*$^{+/min}$ mice (11-keto-corticosterone: 1.16 ± 0.45 vs. 4.56 ± 1.15 ng/g of wild type *Apc*$^{+/min}$ mice, $p < 0.05$). Therefore, selective deletion of 11ßHSD2 in intestinal epithelia was associated with increases in active glucocorticoid levels and decreases in inactive glucocorticoid levels in intestine of Vil-HSD2-/- *Apc*$^{+/min}$ mouse.

To collect enough adenoma tissue for analysis, animals were sacrificed at 20 weeks of age. Immunohistochemistry demonstrated that adenoma epithelial 11ßHSD2 immunostaining was evident in wild type *Apc*$^{+/min}$ mice but diminished in Vil-HSD2-/- *Apc*$^{+/min}$ mice (Figure 2A). In Vil-HSD2-/- *Apc*$^{+/min}$ mouse adenoma epithelia, decreased 11ßHSD2 expression was associated with decreased COX-2 expression. In contrast, adenoma stromal COX-2 expression was comparable between wild type *Apc*$^{+/min}$ mice and Vil-HSD2-/- *Apc*$^{+/min}$ mice (Figure 2B). Immunoblotting confirmed decreased adenoma COX-2 expression in Vil-HSD2-/- *Apc*$^{+/min}$ mice (Figure 2C). Therefore, 11ßHSD2 deletion in adenoma epithelia led to selective COX-2 inhibition in epithelia in Vil-HSD2-/- *Apc*$^{+/min}$ mouse.

At 20 weeks of age, total intestinal adenoma number was markedly lower in Vil-HSD2-/- *Apc*$^{+/min}$ mice than wild type *Apc*$^{+/min}$ mice (44.3 ± 5.3 vs. 83.9 ± 4.9 in wild type, $P < 0.001$, n = 10 in wild type group and n = 8 Vil-HSD2-/- group) (Figure 3). Adenoma size is an independent risk factor for the progression of colorectal cancer (30). Adenomas were stratified by size to determine whether selective deletion of 11ßHSD2 in intestinal epithelia affected size. Vil-HSD2-/- *Apc*$^{+/min}$ mice showed significant decreases in polyps smaller than 2 mm, but had no difference in polyps larger than 2 mm (Figure 3), suggesting that inhibiting intestinal epithelial 11ßHSD2 primarily prevented the initiation of polyp formation.

To determine whether inhibition of tumorigenesis in Vil-HSD2-/- *Apc*$^{+/min}$ mice was related to decreased cell proliferation and/or increased apoptosis, the expression levels of cyclin D1, c-Myc, β-catenin and cleaved caspase-3 were investigated. Immunostaining indicated that cyclin D1 was primarily localized to the nuclei of adenoma epithelial cells. Both cyclin D1 immunostaining density and the number of cyclin D1 positive epithelial cells were reduced in Vil-HSD2-/- *Apc*$^{+/min}$ mice compared to wild type *Apc*$^{+/min}$ mice (Figure 4A). Western blot analysis confirmed the decreased adenoma cyclin D1 expression in Vil-HSD2-/- *Apc*$^{+/min}$ mice. Similarly, the expression levels of adenoma c-Myc and β-catenin were also reduced in Vil-HSD2-/- *Apc*$^{+/min}$ mice (Figure 4 B&C). In contrast, the number of adenoma cells that were positive for cleaved caspase-3, a specific marker of apoptosis, was significantly higher in Vil-HSD2-/- *Apc*$^{+/min}$ mice compared to wild type *Apc*$^{+/min}$ mice (Figure 4 D). Therefore, there was decreased cell proliferation and increased apoptosis in adenomas of Vil-HSD2-/- *Apc*$^{+/min}$ mice.

The retinoblastoma protein (Rb), a tumor suppressor, inhibits cell proliferation through its interaction with the E2F family of transcription factors and the resultant regression of genes that are essential for DNA synthesis (31). The inactivation of retinoblastoma protein is a prerequisite for cell proliferation. Inactivation of Rb is achieved through cyclin-dependent protein kinase-mediated phosphorylation during cell cycle progression. Glucocorticoids activate Rb through p53-mediated induction of p21$^{waf1/cip1}$, an inhibitor of cyclin-dependent kinase (28, 31-35). qRT-PCR determined that both adenoma p53 and p21 mRNA levels increased markedly in Vil-HSD2-/- *Apc*$^{+/min}$ mice compared to wild type *Apc*$^{+/min}$ mice (p53 mRNA: 27.8 ± 3.5 vs. 14.4 ± 2.8 of wild type *Apc*$^{+/min}$ mice, $P < 0.05$; p21$^{waf1/cip1}$ mRNA: 94.1 ± 5.6 vs. 51.7 ± 5.6 of wild type *Apc*$^{+/min}$ mice, $P < 0.001$, n = 6 in each group) (Figure 5A). The expression of adenoma p27, another inhibitor of cyclin-dependent protein kinase, was not affected. Immunostaining demonstrated that p21$^{waf1/cip1}$ in adenomas was predominantly localized to nuclei, and the density of p21$^{waf1/cip1}$ positive cells was markedly higher in Vil-HSD2-/- *Apc*$^{+/min}$ mice than in wild type *Apc*$^{+/min}$ mice (p21$^{waf1/cip1}$ cells/hpf: 41. 3 ± 4.8 vs. 11.8 ± 1.6 of wild type *Apc*$^{+/min}$ mice, $P < 0.001$, n = 4) (Figure 5B). We further found that the phosphorylation levels of retinoblastoma protein in adenomas were dramatically reduced in Vil-HSD2-/- *Apc*$^{+/min}$ mice (Figure 5C). Immunostaining determined that phosphorylated retinoblastoma protein in adenomas was present in nuclei as well as in the cytosol and its expression was reduced in Vil-HSD2-/- *Apc*$^{+/min}$ mice (Figure 5C). Therefore, in Vil-HSD2-/- *Apc*$^{+/min}$ mice, increased active glucocorticoids in adenoma epithelial cells stimulated the signaling pathway regulating retinoblastoma protein mediated cell cycle arrest.

Glucocorticoids may also inhibit tumor growth through suppression of the mTOR signal pathway (36, 37). REDD1 (RTP801, an mTOR complex 1, mTORC1, repressor) is a novel stress-induced gene linked to regression of mTOR signaling and is induced by glucocorticoids (38-40). Therefore, we investigated whether REDD1 expression and activity of mTOR pathway were altered in adenomas from Vil-HSD2-/- *Apc*$^{+/min}$ mice. Adenoma REDD1 mRNA levels were markedly higher in Vil-HSD2-/- *Apc*$^{+/min}$ mice than in wild type *Apc*$^{+/min}$ mice (32.8 ± 2.9 vs. 18.8 ± 2.2 of wild type *Apc*$^{+/min}$, $P < 0.01$, n = 6) (Figure 6A) and adenoma REDD1 protein level was more than 2-folds higher in Vil-HSD2-/- *Apc*$^{+/min}$ mice than in wild type *Apc*$^{+/min}$ mice (Figure 6B). In contrast, the activity of adenoma mTOR pathway was suppressed in Vil-HSD2-/- *Apc*$^{+/min}$ mice as indicated by decreased phosphorylated mTOR (Ser2448) levels (Figure 6C) as well as decreased levels of phosphorylated p70 S6K (Figure 6D) and phosphorylated 4E-BP1 (Figure 6E), two major downstream targets of mTOR signaling. In addition, levels of adenoma phosphorylated S6 ribosomal protein (rpS6, Ser235/236), a downstream target of p70 S6K, were decreased in Vil-HSD2-/- *Apc*$^{+/min}$ mice (Figure 6F). The levels of adenoma phosphorylated eEF2K,

another downstream target of p70 S6K, were also reduced in Vil-HSD2-/- $Apc^{+/min}$ mice (data not shown).

To investigate whether inhibition of the COX-2 pathway contributes to cell cycle arrest and suppression of mTOR pathway seen in Vil-HSD2-/- $Apc^{+/min}$ mice, wild type $Apc^{+/min}$ mice were treated with a selective COX-2 inhibitor and activity of retinoblastoma protein and mTOR was determined. As indicated in Supplementary Figure 3, inhibition of COX-2 pathway had no effect on activity of mTOR (Ser2448) and retinoblastoma protein. In cultured mouse colon adenocarcinoma MC-38 cells, treatment with dexamethasone, a synthetic glucocorticoid, led to induction of p53, p21 and REDD1 (supplemental Figure 4A) but inhibition of the phosphorylation of retinoblastoma protein, mTOR (Ser2448), and p70 S6K, all of which were reversed by the glucocorticoid receptor inhibitor, RU486 (Supplementary Figure 4B), indicating that glucocorticoids may inhibit colon cancer cell proliferation through activating the tumor suppressor retinoblastoma protein pathway and inhibiting the mTOR pathway. In addition, inhibition of mTOR activity or inhibition of COX-2 activity did not affect the expression levels of p53, p21 and REDD1 in MC38 cells (Supplemental Figure 5).

Discussion

Our present results demonstrate that intestinal epithelial 11ßHSD2 activity contributes to increased COX-2 expression in $Apc^{+/min}$ mouse intestinal adenomas and that 11ßHSD2 deficiency in intestinal epithelial cells suppresses adenoma development and growth due to inhibition of the COX-2 pathway, induction of G1 cell cycle arrest, and inhibition of the mTOR pathway as a result of increased intracellular active glucocorticoids in tumor epithelial cells (Figure 7). Recent studies have demonstrated a clear molecular link between COX-2-derived PGE_2 and colorectal cancer progression (1), and inhibition of COX-2-derived PGE_2 production by traditional NSAIDs or selective COX-2 inhibitors reduces the number and size of adenomas in $Apc^{+/min}$ mice and in FAP patients (3-6),(10,11,28). However, increased gastrointestinal side effects of traditional NSAIDs and increased cardiovascular risks of selective COX-2 inhibitors limit their use in chemoprevention of CRC. That most patients present with advanced disease and that metastatic disease is largely incurable underscore that prevention remains the best approach to reduce the overall morbidity and mortality of CRC.

GCs and NSAIDs inhibit prostaglandin biosynthesis through different mechanisms. NSAIDs inhibit prostaglandin biosynthesis by non-competitive inhibition of both COX-1 and COX-2 enzymatic activity. GCs are the most potent, endogenous, specific COX-2 inhibitors. GCs suppress prostaglandin production through inhibiting cytosolic phospholipase A_2 activity and suppressing COX-2 and mPGES-1 expression. The actions of GCs are regulated systemically and locally (7). Circulating glucocorticoid levels are regulated by the hypothalamo-pituitary-adrenal axis. Within target tissues, the actions of GCs are down-regulated by 11ßHSD2-mediated metabolism. 11ßHSD2 is expressed predominantly in mineralocorticoid responsive tissues such as the kidney and colon to convert GCs to their inactive keto-forms, thus providing mineralocorticoid receptor selectivity to aldosterone.

GCs are known to inhibit cell proliferation and induce cell differentiation through activation of glucocorticoid receptors. 11ßHSD2 has been thought to be pro-proliferative due to its ability to inactivate glucocorticoids (41,44). We recently reported that 11ßHSD2 expression is increased in epithelial cells and stromal cells in human colonic and $Apc^{+/min}$ mouse intestinal adenomas and is correlated with increased COX-2 expression and activity, and that inhibition of 11ßHSD2 activity with glycyrrhizic acid suppresses tumor COX-2 pathway and prevents adenoma formation, tumor growth, and metastasis as a result of increased tumor

intracellular active glucocorticoids (23). One limitation of our previous study is that glycyrrhizic acid is not a specific 11ßHSD2 inhibitor, and its potential off-target effects could not be excluded. The other limitation is that pharmacologic inhibition of 11ßHSD2 activity cannot distinguish the role of epithelial vs. stromal 11ßHSD2 in tumorigenesis.

In the current studies, we generated *Apc*$^{+/min}$ mice with selective deletion of 11ßHSD2 in intestinal epithelia, Vil-HSD2-/- *Apc*$^{+/min}$ mice, which had reduced 11ßHSD2 and COX-2 expression with concomitant increased active corticosterone levels and decreased inactive 11-keto-corticosterone levels in the intestine (Figure 1). In adenomas from Vil-HSD2-/- *Apc*$^{+/min}$ mouse, both epithelial 11ßHSD2 and COX-2 expression decreased, while stromal COX-2 expression was not affected. Therefore, in Vil-HSD2-/- *Apc*$^{+/min}$ mouse adenomas, selective deletion of 11ßHSD2 in epithelia was associated with selective inhibition of COX-2 that was confined to the epithelia. In Vil-HSD2-/- *Apc*$^{+/min}$ mouse, epithelial 11ßHSD2 and COX-2 deficiency was associated with a marked decrease in total adenoma number while the number of adenomas larger than 2 mm was not affected, suggesting that epithelial 11ßHSD2 and/or COX-2 may primarily promote the initiation and formation of adenomas or that in large adenomas 11ßHSD2 was not sufficiently deleted. Since COX-2 inhibitors and COX-2 deletion dramatically decrease both adenoma formation and size (10, 11, 28, 45), the present results suggested that the stroma may be the major source of prostaglandins that mediate adenoma growth (46). Treatment with a peroxisome proliferator-activated receptor-δ agonist primarily increases intestinal adenoma growth in *Apc*$^{+/min}$ mice (30), further suggesting that *Apc*$^{+/min}$ mouse intestinal adenoma development and growth may be regulated by different signal pathways.

A recent study with overexpression of COX-2 in intestinal epithelia suggests that increased intestinal epithelial COX-2 is not itself sufficient to initiate tumorigenesis (47). In Vil-HSD2-/- *Apc*$^{+/min}$ mouse, tumorigenesis was markedly inhibited, although only epithelial COX-2 expression was decreased, suggesting involvement of further signaling pathways. Indeed, increased intracellular active glucocorticoids in epithelia after 11ßHSD2 deletion could inhibit cell proliferation and induce differentiation through different mechanisms such as induction of G1 cell cycle arrest and inhibition of the mTOR pathway (36-38, 48).

Glucocorticoids induce G1 cell cycle arrest through p-53 mediated induction of p21$^{waf1/cip1}$, known as a cyclin-dependent kinase inhibitor, which directly binds to and inhibits the activity of cyclin E/CDK2 and cylin D/CDK4/6 complexes, leading to hypophosphorylation of its major downstream target, the retinoblastoma protein, a tumor suppressor. Activated Rb due to dephosphorylation interacts with the E2F family of transcription factors and inhibits cell cycle progression (31). In adenomas from Vil-HSD2-/- *Apc*$^{+/min}$ mouse, p53 and p21$^{waf1/cip1}$ levels were markedly increased while the levels of phosphorylated Rb were decreased, suggesting G1 cell cycle arrest contributes to tumor inhibition due to 11ßHSD2 deletion in epithelia as a result of increased intracellular active glucocorticoids. mTOR signaling is critical in cell growth (49). REDD1 is an mTOR inhibitor and has been found to be upregulated in several colon cancer cell lines when their growth is inhibited (50). Glucocorticoids have been reported to inhibit the mTOR pathway through induction of REDD1 (38-40). In adenomas from Vil-HSD2-/- *Apc*$^{+/min}$ mouse, both REDD1 mRNA and protein levels increased, while activity of the mTOR pathway was inhibited as indicated by decreased phosphorylation of mTOR (Ser2448), p70-S6K, 4E-BP1, and S6 ribosomal protein (Figure 6).

The current investigation supports our previous studies that suggested that inhibition of 11ßHSD2 activity with glycyrrhizic acid and its analogs may represent a novel approach for CRC chemoprevention with the following advantages by increasing tumor active glucocorticoids: 1) GCs selectively inhibit the COX-2 but not COX-1 pathway, therefore

having the beneficial effects of traditional NSAIDs to prevent and regress colorectal cancers without the gastrointestinal side-effects associated with COX-1 inhibition; 2) Physiologic 11ßHSD2 expression is largely restricted to colon and kidney. Therefore, inhibition of 11ßHSD2 activity is not expected to incur the cardiovascular risk posed by COX-2 inhibitors that suppress COX-2-derived PGI_2 production in vascular endothelial cells; 3) Intracellular active GCs are only increased in tissues with elevated 11ßHSD2 expression. 11ßHSD2 inhibition will not produce immunosuppression or other systemic side-effects of conventional glucocorticoid therapy; 4) In addition to inhibiting the COX-2 pathway, increased tumor active GCs also inhibit tumor development and growth through induction of G1 cell cycle arrest and inhibition of the mTOR pathway (Figure 7). Although 11ßHSD2 inhibition may result in salt-dependent hypertension due to activation of mineralocorticoid receptors by GCs, development of locally acting enteric 11ßHSD2 inhibitors that are not systemically absorbed would be a potential therapeutic means to prevent colorectal tumorigenesis (7).

Supplementary Material

Refer to Web version on PubMed Central for supplementary material.

Acknowledgments

Grant Support

These studies were supported by grants from the National Institutes of Health (CA122620, DK38226, DK51265, DK62794, GM15431, ES13125, NCI P50 95103 Special Program of Research Excellence), by the Vanderbilt O'Brien Center (DK79341), by funds from the Veterans Administration, by grant from National Natural Science Foundation of China (31170809), by National Key Basic Research Program of China (973 Program, #2012CB524900) and by Hundred Talents Program from CAS (2012OHTP07).

References

1. Castellone MD, Teramoto H, Williams BO, Druey KM, Gutkind JS. Prostaglandin E2 promotes colon cancer cell growth through a Gs-axin-beta-catenin signaling axis. Science. 2005; 310:1504–10. [PubMed: 16293724]
2. Wang D, Dubois RN. Eicosanoids and cancer. Nat Rev Cancer. 2010; 10:181–93. [PubMed: 20168319]
3. Baron JA, Cole BF, Sandler RS, Haile RW, Ahnen D, Bresalier R, et al. A randomized trial of aspirin to prevent colorectal adenomas. N Engl J Med. 2003; 348:891–9. [PubMed: 12621133]
4. Giovannucci E, Egan KM, Hunter DJ, Stampfer MJ, Colditz GA, Willett WC, et al. Aspirin and the risk of colorectal cancer in women. N Engl J Med. 1995; 333:609–14. [PubMed: 7637720]
5. Rosenberg L, Louik C, Shapiro S. Nonsteroidal antiinflammatory drug use and reduced risk of large bowel carcinoma. Cancer. 1998; 82:2326–33. [PubMed: 9635524]
6. Thun MJ, Namboodiri MM, Heath CW Jr. Aspirin use and reduced risk of fatal colon cancer. N Engl J Med. 1991; 325:1593–6. [PubMed: 1669840]
7. Stewart PM, Prescott SM. Can licorice lick colon cancer? J Clin Invest. 2009; 119:760–3. [PubMed: 19348044]
8. Dannenberg AJ, Altorki NK, Boyle JO, Dang C, Howe LR, Weksler BB, et al. Cyclo-oxygenase 2: a pharmacological target for the prevention of cancer. Lancet Oncol. 2001; 2:544–51. [PubMed: 11905709]
9. Gwyn K, Sinicrope FA. Chemoprevention of colorectal cancer. Am J Gastroenterol. 2002; 97:13–21. [PubMed: 11808936]
10. Steinbach G, Lynch PM, Phillips RK, Wallace MH, Hawk E, Gordon GB, et al. The effect of celecoxib, a cyclooxygenase-2 inhibitor, in familial adenomatous polyposis. N Engl J Med. 2000; 342:1946–52. [PubMed: 10874062]

11. Jacoby RF, Seibert K, Cole CE, Kelloff G, Lubet RA. The cyclooxygenase-2 inhibitor celecoxib is a potent preventive and therapeutic agent in the min mouse model of adenomatous polyposis. Cancer Res. 2000; 60:5040–4. [PubMed: 11016626]
12. Bresalier RS, Sandler RS, Quan H, Bolognese JA, Oxenius B, Horgan K, et al. Cardiovascular events associated with rofecoxib in a colorectal adenoma chemoprevention trial. N Engl J Med. 2005; 352:1092–102. [PubMed: 15713943]
13. Solomon SD, McMurray JJ, Pfeffer MA, Wittes J, Fowler R, Finn P, et al. Cardiovascular risk associated with celecoxib in a clinical trial for colorectal adenoma prevention. N Engl J Med. 2005; 352:1071–80. [PubMed: 15713944]
14. Cheng Y, Austin SC, Rocca B, Koller BH, Coffman TM, Grosser T, et al. Role of prostacyclin in the cardiovascular response to thromboxane A2. Science. 2002; 296:539–41. [PubMed: 11964481]
15. Clark AR, Lasa M. Crosstalk between glucocorticoids and mitogen-activated protein kinase signalling pathways. Curr Opin Pharmacol. 2003; 3:404–11. [PubMed: 12901950]
16. Newton R. Molecular mechanisms of glucocorticoid action: what is important? Thorax. 2000; 55:603–13. [PubMed: 10856322]
17. Zhang MZ, Harris RC, McKanna JA. Regulation of cyclooxygenase-2 (COX-2) in rat renal cortex by adrenal glucocorticoids and mineralocorticoids. Proc Natl Acad Sci U S A. 1999; 96:15280–5. [PubMed: 10611376]
18. Croxtall JD, Gilroy DW, Solito E, Choudhury Q, Ward BJ, Buckingham JC, et al. Attenuation of glucocorticoid functions in an Anx-A1-/- cell line. Biochem J. 2003; 371:927–35. [PubMed: 12553880]
19. Stichtenoth DO, Thoren S, Bian H, Peters-Golden M, Jakobsson PJ, Crofford LJ. Microsomal prostaglandin E synthase is regulated by proinflammatory cytokines and glucocorticoids in primary rheumatoid synovial cells. J Immunol. 2001; 167:469–74. [PubMed: 11418684]
20. Denis MG, Chadeneau C, Blanchardie P, Lustenberger P. Biological effects of glucocorticoid hormones on two rat colon adenocarcinoma cell lines. J Steroid Biochem Mol Biol. 1992; 41:739–45. [PubMed: 1562548]
21. Schiffelers RM, Metselaar JM, Fens MH, Janssen AP, Molema G, Storm G. Liposome-encapsulated prednisolone phosphate inhibits growth of established tumors in mice. Neoplasia. 2005; 7:118–27. [PubMed: 15802017]
22. Funder JW, Pearce PT, Smith R, Smith AI. Mineralocorticoid action: target tissue specificity is enzyme, not receptor, mediated. Science. 1988; 242:583–5. [PubMed: 2845584]
23. Zhang MZ, Xu J, Yao B, Yin H, Cai Q, Shrubsole MJ, et al. Inhibition of 11beta-hydroxysteroid dehydrogenase type II selectively blocks the tumor COX-2 pathway and suppresses colon carcinogenesis in mice and humans. J Clin Invest. 2009; 119:876–85. [PubMed: 19307727]
24. Madison BB, Dunbar L, Qiao XT, Braunstein K, Braunstein E, Gumucio DL. Cis elements of the villin gene control expression in restricted domains of the vertical (crypt) and horizontal (duodenum, cecum) axes of the intestine. J Biol Chem. 2002; 277:33275–83. [PubMed: 12065599]
25. Su LK, Kinzler KW, Vogelstein B, Preisinger AC, Moser AR, Luongo C, et al. Multiple intestinal neoplasia caused by a mutation in the murine homolog of the APC gene. Science. 1992; 256:668–70. [PubMed: 1350108]
26. Zhang MZ, Yao B, Cheng HF, Wang SW, Inagami T, Harris RC. Renal cortical cyclooxygenase 2 expression is differentially regulated by angiotensin II AT(1) and AT(2) receptors. Proc Natl Acad Sci U S A. 2006; 103:16045–50. [PubMed: 17043228]
27. Zhang B, Halder SK, Kashikar ND, Cho YJ, Datta A, Gorden DL, et al. Antimetastatic role of Smad4 signaling in colorectal cancer. Gastroenterology. 2010; 138:969–80. [PubMed: 19909744]
28. Harris RC, McKanna JA, Akai Y, Jacobson HR, Dubois RN, Breyer MD. Cyclooxygenase-2 is associated with the macula densa of rat kidney and increases with salt restriction. J Clin Invest. 1994; 94:2504–10. [PubMed: 7989609]
29. Shao J, Washington MK, Saxena R, Sheng H. Heterozygous disruption of the PTEN promotes intestinal neoplasia in APCmin/+ mouse: roles of osteopontin. Carcinogenesis. 2007; 28:2476–83. [PubMed: 17693663]

30. Gupta RA, Wang D, Katkuri S, Wang H, Dey SK, DuBois RN. Activation of nuclear hormone receptor peroxisome proliferator-activated receptor-delta accelerates intestinal adenoma growth. Nat Med. 2004; 10:245–7. [PubMed: 14758356]

31. Chau BN, Wang JY. Coordinated regulation of life and death by RB. Nat Rev Cancer. 2003; 3:130–8. [PubMed: 12563312]

32. Cram EJ, Ramos RA, Wang EC, Cha HH, Nishio Y, Firestone GL. Role of the CCAAT/enhancer binding protein-alpha transcription factor in the glucocorticoid stimulation of p21waf1/cip1 gene promoter activity in growth-arrested rat hepatoma cells. J Biol Chem. 1998; 273:2008–14. [PubMed: 9442037]

33. Cha HH, Cram EJ, Wang EC, Huang AJ, Kasler HG, Firestone GL. Glucocorticoids stimulate p21 gene expression by targeting multiple transcriptional elements within a steroid responsive region of the p21waf1/cip1 promoter in rat hepatoma cells. J Biol Chem. 1998; 273:1998–2007. [PubMed: 9442036]

34. Reil TD, Kashyap VS, Sarkar R, Freishlag J, Gelabert HA. Dexamethasone inhibits the phosphorylation of retinoblastoma protein in the suppression of human vascular smooth muscle cell proliferation. J Surgl Res. 2000; 92:108–13.

35. Addeo R, Casale F, Caraglia M, D'Angelo V, Crisci S, Abbruzzese A, et al. Glucocorticoids induce G1 arrest of lymphoblastic cells through retinoblastoma protein Rb1 dephosphorylation in childhood acute lymphoblastic leukemia in vivo. Cancer Biol Ther. 2004; 3:470–6. [PubMed: 15034294]

36. Polman JA, Hunter RG, Speksnijder N, van den Oever JM, Korobko OB, McEwen BS, et al. Glucocorticoids Modulate the mTOR Pathway in the Hippocampus: Differential Effects Depending on Stress History. Endocrinology. 2012; 153:4317–27. [PubMed: 22778218]

37. Shimizu N, Yoshikawa N, Ito N, Maruyama T, Suzuki Y, Takeda S, et al. Crosstalk between glucocorticoid receptor and nutritional sensor mTOR in skeletal muscle. Cell Metab. 2011; 13:170–82. [PubMed: 21284984]

38. Wang H, Kubica N, Ellisen LW, Jefferson LS, Kimball SR. Dexamethasone represses signaling through the mammalian target of rapamycin in muscle cells by enhancing expression of REDD1. J Biol Chem. 2006; 281:39128–34. [PubMed: 17074751]

39. Molitoris JK, McColl KS, Swerdlow S, Matsuyama M, Lam M, Finkel TH, et al. Glucocorticoid elevation of dexamethasone-induced gene 2 (Dig2/RTP801/REDD1) protein mediates autophagy in lymphocytes. J Biol Chem. 2011; 286:30181–9. [PubMed: 21733849]

40. Kumari R, Willing LB, Jefferson LS, Simpson IA, Kimball SR. REDD1 (regulated in development and DNA damage response 1) expression in skeletal muscle as a surrogate biomarker of the efficiency of glucocorticoid receptor blockade. Biochem Biophys Res Commun. 2011; 412:644–7. [PubMed: 21856283]

41. Rabbitt EH, Gittoes NJ, Stewart PM, Hewison M. 11beta-hydroxysteroid dehydrogenases, cell proliferation and malignancy. J Steroid Biochem Mol Biol. 2003; 85:415–21. [PubMed: 12943730]

42. Hundertmark S, Buhler H, Rudolf M, Weitzel HK, Ragosch V. Inhibition of 11 beta-hydroxysteroid dehydrogenase activity enhances the antiproliferative effect of glucocorticosteroids on MCF-7 and ZR-75-1 breast cancer cells. J Endocrinol. 1997; 155:171–80. [PubMed: 9390020]

43. Lipka C, Mankertz J, Fromm M, Lubbert H, Buhler H, Kuhn W, et al. Impairment of the antiproliferative effect of glucocorticosteroids by 11beta-hydroxysteroid dehydrogenase type 2 overexpression in MCF-7 breast-cancer cells. Horm Metab Res. 2004; 36:437–44. [PubMed: 15305225]

44. Koyama K, Myles K, Smith R, Krozowski Z. Expression of the 11beta-hydroxysteroid dehydrogenase type II enzyme in breast tumors and modulation of activity and cell growth in PMC42 cells. J Steroid Biochem Mol Biol. 2001; 76(1-5):153–9. [PubMed: 11384873]

45. Chulada PC, Thompson MB, Mahler JF, Doyle CM, Gaul BW, Lee C, et al. Genetic disruption of Ptgs-1, as well as Ptgs-2, reduces intestinal tumorigenesis in Min mice. Cancer Res. 2000; 60:4705–8. [PubMed: 10987272]

46. Hull MA, Booth JK, Tisbury A, Scott N, Bonifer C, Markham AF, et al. Cyclooxygenase 2 is up-regulated and localized to macrophages in the intestine of Min mice. Br J Cancer. 1999; 79:1399–405. [PubMed: 10188882]

47. Al-Salihi MA, Terrece Pearman A, Doan T, Reichert EC, Rosenberg DW, Prescott SM, et al. Transgenic expression of cyclooxygenase-2 in mouse intestine epithelium is insufficient to initiate tumorigenesis but promotes tumor progression. Cancer Lett. 2009; 273:225–32. [PubMed: 18790560]

48. Zoncu R, Efeyan A, Sabatini DM. mTOR: from growth signal integration to cancer, diabetes and ageing. Nat Rev Mol Cell Biol. 2011; 12:21–35. [PubMed: 21157483]

49. Laplante M, Sabatini DM. mTOR signaling in growth control and disease. Cell. 2012; 149:274–93. [PubMed: 22500797]

50. Protiva P, Hopkins ME, Baggett S, Yang H, Lipkin M, Holt PR, et al. Growth inhibition of colon cancer cells by polyisoprenylated benzophenones is associated with induction of the endoplasmic reticulum response. Int J Cancer. 2008; 123:687–94. [PubMed: 18470880]

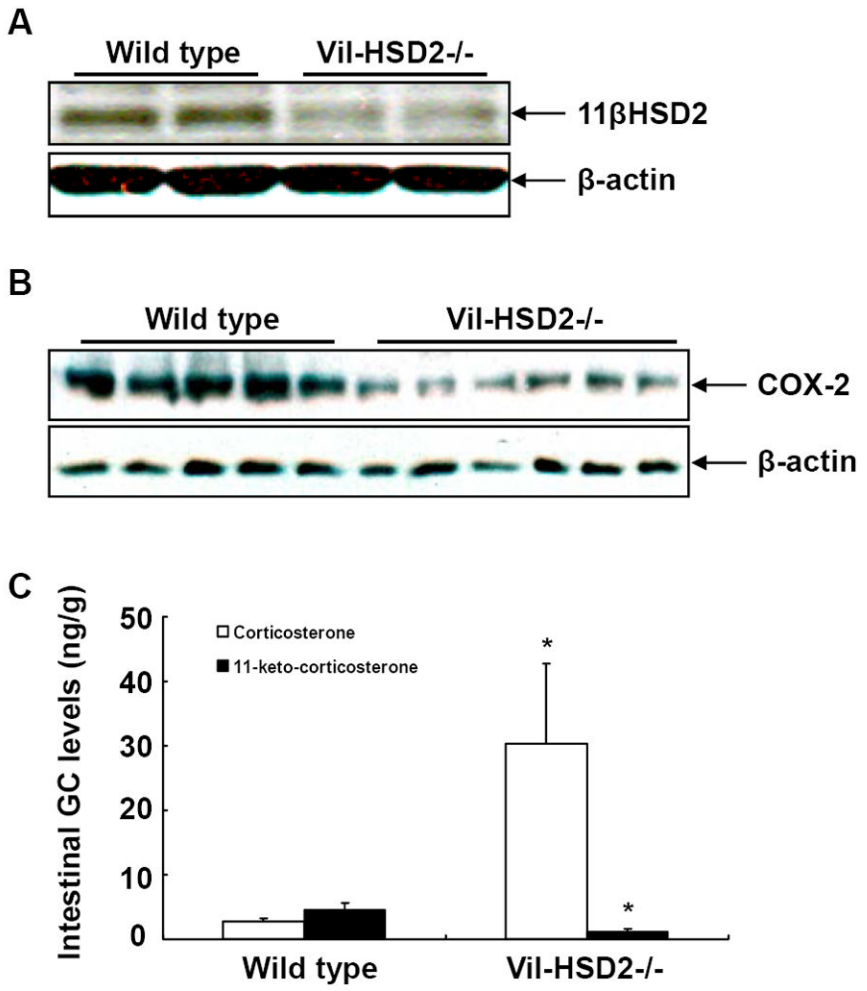

Figure 1. Intestinal 11ßHSD2 and COX-2 expression decreased in Vil-HSD2-/- *Apc*$^{+/min}$ mice

(**A**) Immunoblotting indicated decreased intestinal 11ßHSD2 expression in Vil-HSD2-/- *Apc*$^{+/min}$ mice compared to wild type *Apc*$^{+/min}$ mice. (**B**) Immunoblotting demonstrated decreased intestinal COX-2 expression in Vil-HSD2-/- *Apc*$^{+/min}$ mice (5 wild type mice and 6 Vil-HSD2-/- mice). (**C**) 11ßHSD2 deletion in intestinal epithelia significantly increased corticosterone levels and decreased 11-keto-corticosterone levels in intestines. n = 6. **P* < 0.05 vs. wild type *Apc*$^{+/min}$ mice.

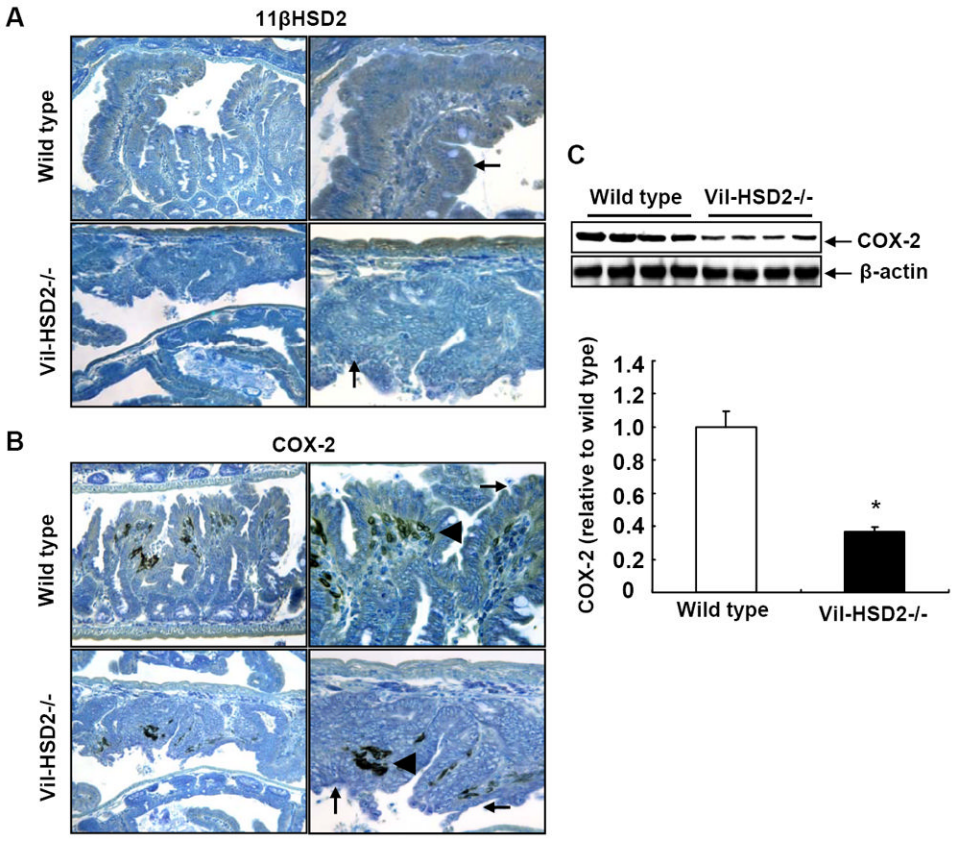

Figure 2. Adenoma epithelial cell 11ßHSD2 and COX-2 expression decreased in Vil-HSD2-/- *Apc*$^{+/min}$ mice

(**A**) Immunostaining indicated that 11ßHSD2 expression in adenoma epithelial cells disappeared in Vil-HSD2-/- *Apc*$^{+/min}$ mice (arrow). Original magnification: Left lanes: × 100; right lanes: × 250. (**B**) Adenoma COX-2 expression disappeared in epithelial cells (arrow), but was still apparent in stromal cells (arrow head) in Vil-HSD2-/- *Apc*$^{+/min}$ mice. Original magnification: Left lanes: × 100; right lanes: × 250. (**C**) Western blot analysis demonstrated decreased adenoma COX-2 expression in Vil-HSD2-/- *Apc*$^{+/min}$ mice. n = 4. **P* < 0.01 vs. wild type *Apc*$^{+/min}$ mice.

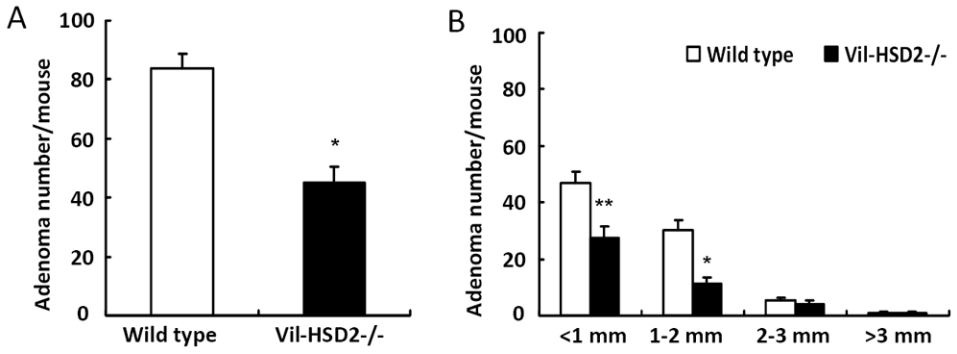

Figure 3. Selective deletion of 11ßHSD2 in intestinal epithelia inhibited tumorigenesis in *Apc*$^{+/min}$ mice

(**A**) 11ßHSD2 deletion in intestinal epithelia led to markedly reduced intestinal adenoma multiplicity (*$P < 0.001$ vs. wild type *Apc*$^{+/min}$ mice, n = 10 in wild type group, n = 8 in Vil-HSD2-/- group). (**B**) Adenomas smaller than 2 mm decreased significantly in Vil-HSD2-/- *Apc*$^{+/min}$ mice (*$P < 0.001$, ** $P < 0.01$ vs. wild type *Apc*$^{+/min}$ mice).

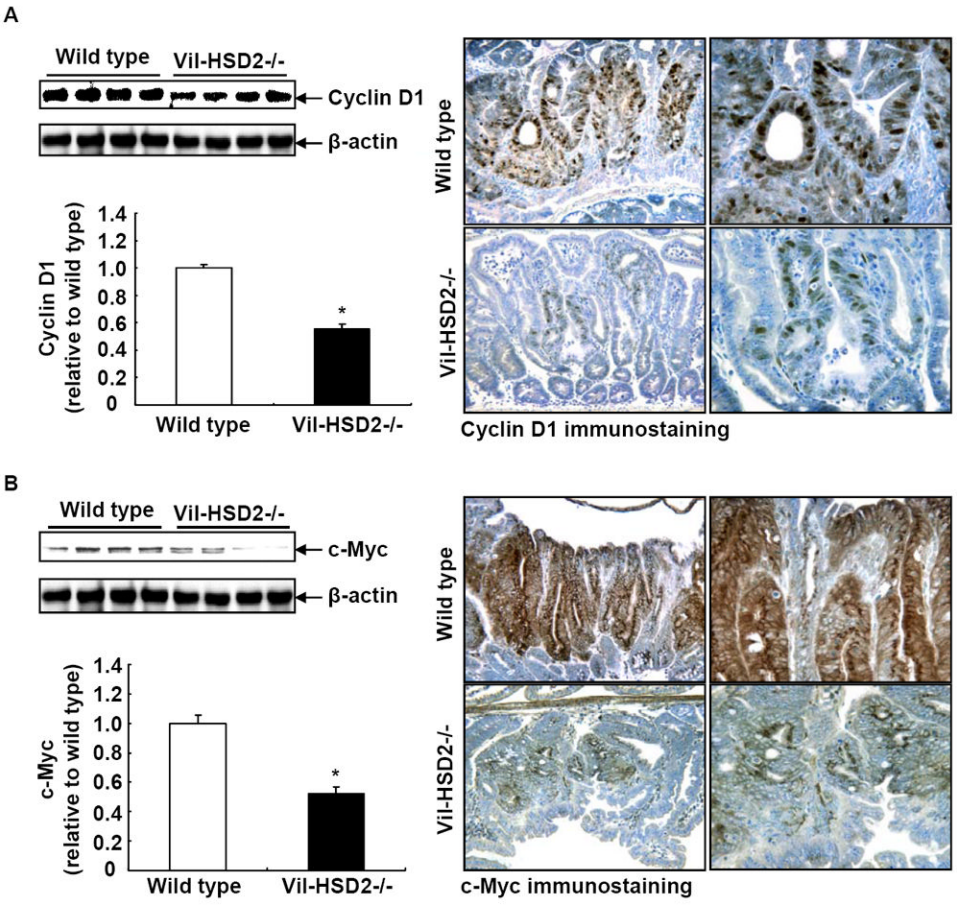

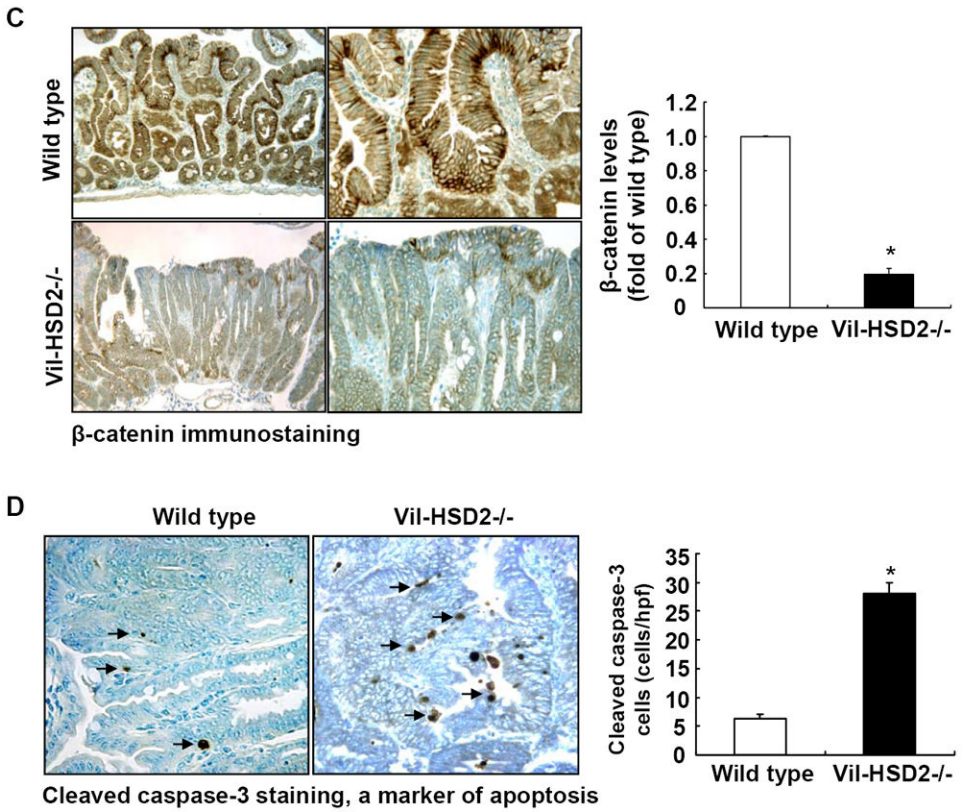

Figure 4. Selective deletion of 11ßHSD2 in intestinal epithelia decreased tumor cell proliferation and increased tumor cell apoptosis

(**A**) Western blot showed decreased cyclin D1 expression in adenomas from Vil-HSD2-/- $Apc^{+/min}$ mice (*$P < 0.01$ vs. wild type $Apc^{+/min}$ mice, n = 4). Immunostaining demonstrated that cyclin D1 was primarily localized to adenoma epithelial cell nuclei, and its expression decreased in Vil-HSD2-/- $Apc^{+/min}$ mice. (**B**) Western blot indicated decreased c-Myc expression in adenomas from Vil-HSD2-/- $Apc^{+/min}$ mice (*$P < 0.01$ vs. wild type $Apc^{+/min}$ mice, n = 4). Immunostaining demonstrated that c-Myc was expressed in nuclei and cytosols in adenoma epithelial cells and its expression decreased in Vil-HSD2-/- $Apc^{+/min}$ mice. (**C**) Immunostaining demonstrated that adenoma ß-catenin expression was markedly inhibited in Vil-HSD2-/- $Apc^{+/min}$ mice compared to wild type $Apc^{+/min}$ mice (*$P < 0.01$ vs. wild type $Apc^{+/min}$ mice, n = 4). (**D**) Adenoma apoptosis increased in Vil-HSD2-/- $Apc^{+/min}$ mice as indicated by increase in cleaved-caspase-3 positive cells, a specific marker of apoptosis (*$P < 0.01$ vs. wild type $Apc^{+/min}$ mice, n = 4). Original magnification: × 100 in left panels of A, B, and C; × 250 in right panels of A, B, and C as well as in D.

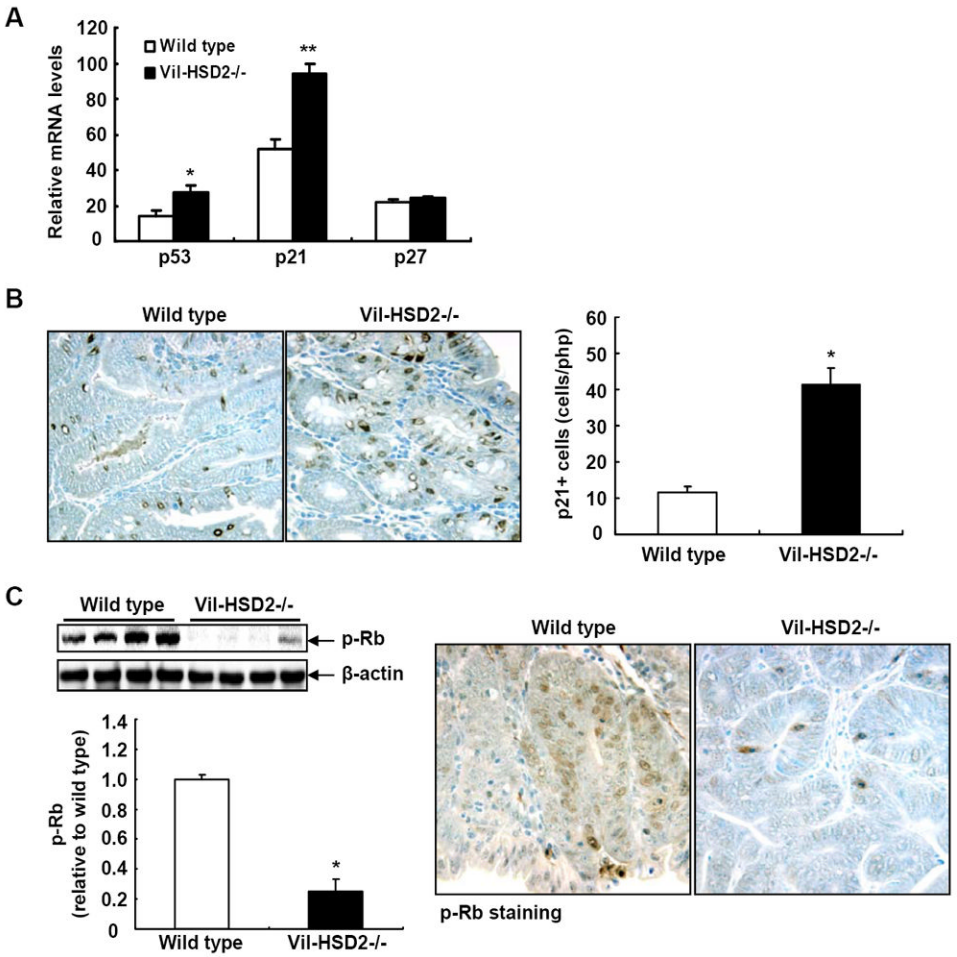

Figure 5. Selective deletion of 11ßHSD2 in intestinal epithelia activated adenoma retinoblastoma protein pathway in *Apc*$^{+/min}$ mice

(**A**) Adenoma mRNA levels of p53 and p21$^{waf1/cip1}$ were increased in Vil-HSD2-/- *Apc*$^{+/min}$ mice (*$P < 0.01$, **$P < 0.05$ versus wild type *Apc*$^{+/min}$ mice, n = 6). (**B**) The number of adenoma p21$^{waf1/cip1}$ positive cells markedly increased in Vil-HSD2-/- *Apc*$^{+/min}$ mice (*$P <$ 0.01, vs. wild type *Apc*$^{+/min}$ mice, n = 4). (**C**) The levels of the active form of the tumor suppressor, retinoblastoma protein (Rb) increased in adenomas from Vil-HSD2-/- *Apc*$^{+/min}$ mice as indicated by decreased phosphorylation (*$P < 0.01$ vs. wild type *Apc*$^{+/min}$ mice, n = 4). Immunostaining confirmed decreased number of phosphorylated Rb positive cells in adenomas from Vil-HSD2-/- *Apc*$^{+/min}$ mice. Original magnification: × 250.

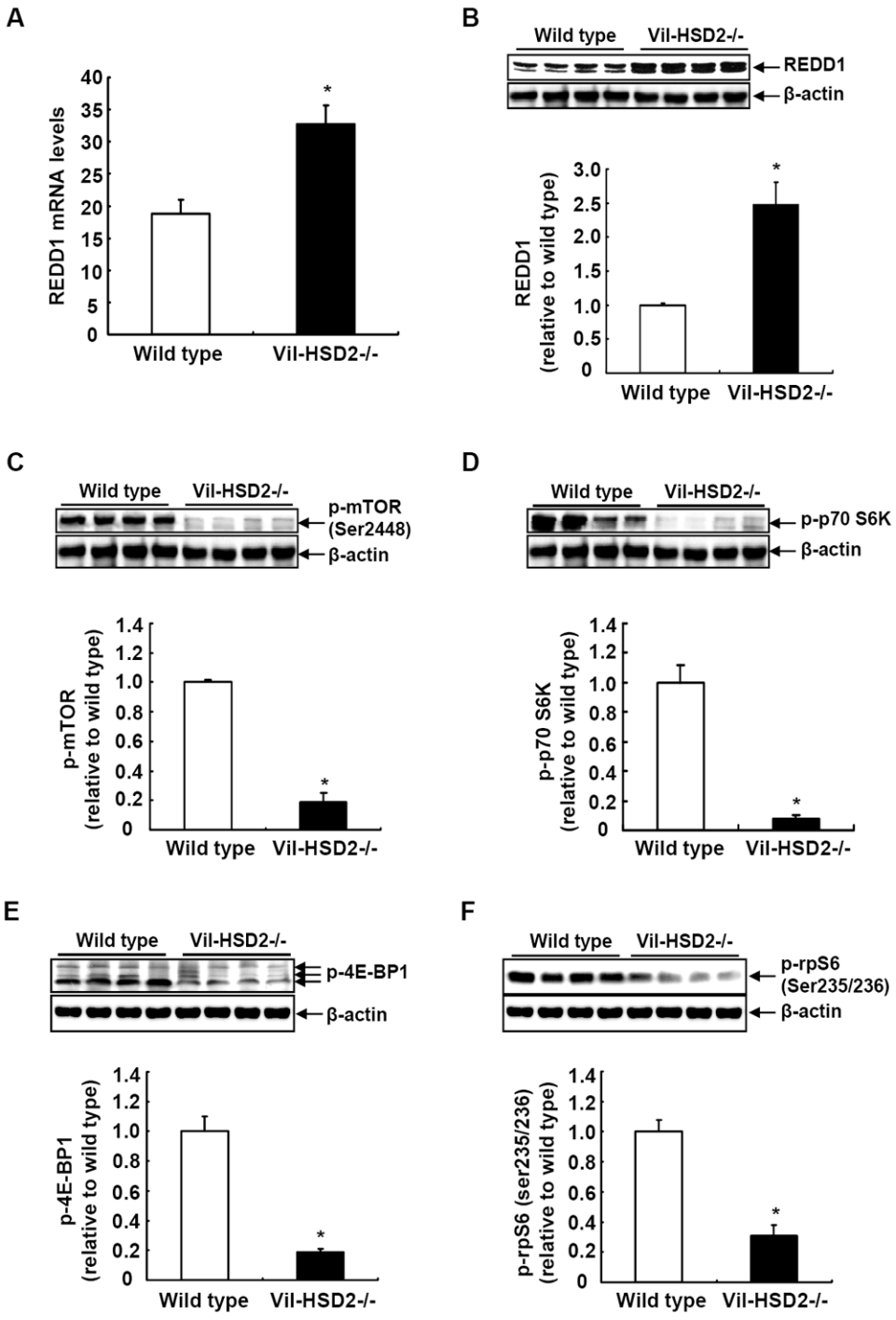

Figure 6. Selective deletion of 11ßHSD2 in intestinal epithelia inhibited adenoma activity of the mTOR pathway in *Apc*$^{+/min}$ mice

(**A**) Adenoma REDD1 mRNA levels were increased in Vil-HSD2-/- *Apc*$^{+/min}$ mice (*$P <$ 0.01 vs. wild type *Apc*$^{+/min}$ mice, n = 6). (**B**) Adenoma REDD1 protein levels were increased in Vil-HSD2-/- *Apc*$^{+/min}$ mice (*$P < 0.01$ vs. wild type *Apc*$^{+/min}$ mice, n = 4). (**C**) Adenoma mTOR activity was markedly inhibited in Vil-HSD2-/- *Apc*$^{+/min}$ mice (*$P < 0.01$ vs. wild type *Apc*$^{+/min}$ mice, n = 4). (**D&E**) Adenoma p-70 S6K and 4E-BP1 activities were

markedly inhibited in Vil-HSD2-/- $Apc^{+/min}$ mice (*$P < 0.01$ vs. wild type $Apc^{+/min}$ mice, n = 4). (**F**) Adenoma levels of phosphorylated S6 ribosomal protein (p-rpS6) were markedly inhibited in Vil-HSD2-/- $Apc^{+/min}$ mice (*$P < 0.01$ vs. wild type $Apc^{+/min}$ mice, n = 4).

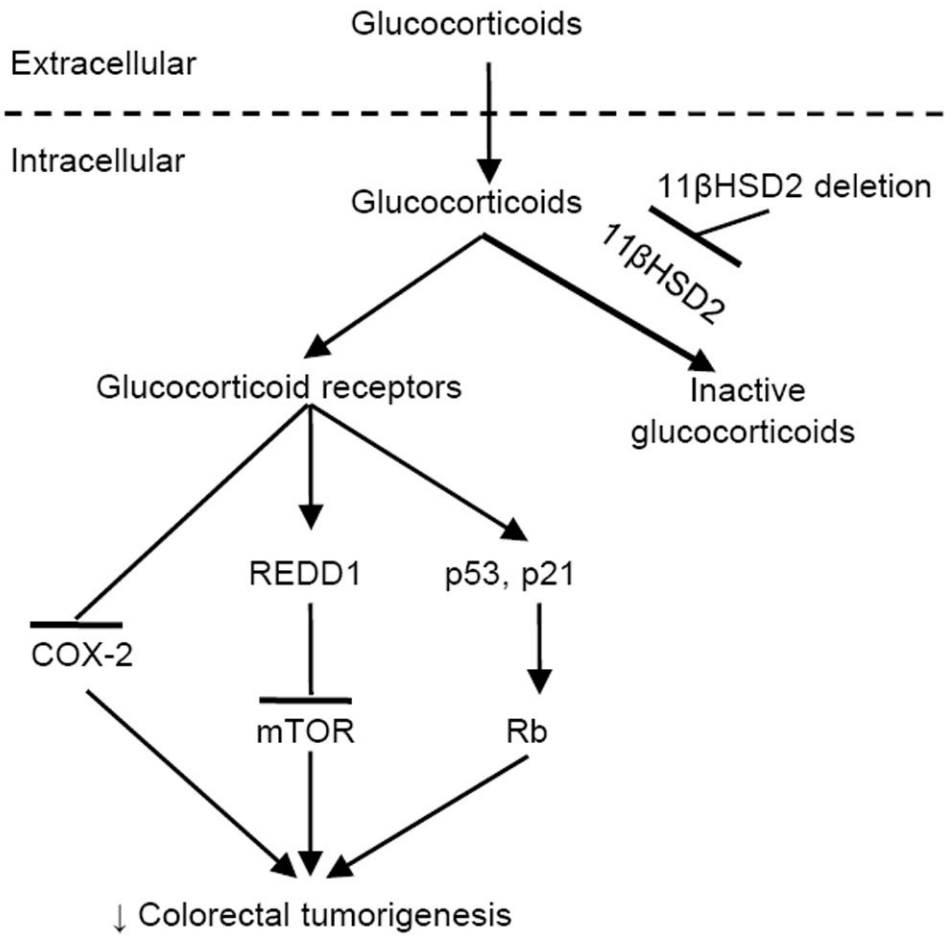

Figure 7. Proposed mechanism underlying epithelial cell 11ßHSD2 activity and colorectal tumorigenesis

In tumor epithelial cells, glucocorticoids are converted to inactive 11-keto-forms, reducing glucocorticoid receptor activity, while 11ßHSD2 deletion leads to increased levels of epithelial intracellular active glucocorticoid. The subsequent inhibition of the COX-2 pathway and induction of G1 cell cycle arrest through activation of retinoblastoma protein (Rb, a tumor suppressor) due to induction of p53 and p21 and inhibition of the mTOR pathway due to induction of REDD1 lead to inhibition of colorectal tumorigenesis.